

# Investigation of the ASTM International frost heave testing method using a temperature-controllable cell

Hyunwoo Jin<sup>a</sup>, Janguen Lee and Byung-Hyun Ryu\*

Department of Future and Smart Construction Research, KICT, 283, Goyang-daero, Ilsanseo-gu,  
Goyang-si, Gyeonggi-do, Republic of Korea

(Received September 19, 2022, Revised November 20, 2022, Accepted December 12, 2022)

**Abstract.** Frost heave can cause uneven ground uplift that may damage geo-infrastructure. To assist damage-prevention strategies, standard frost heave testing methods and frost susceptibility criteria have been established and used in various countries. ASTM International standard testing method is potentially the most useful standard, as abundant experimental data have been acquired through its use. ASTM International provides detailed recommendations, but the method is expensive and laborious because of the complex testing procedure requiring a freezing chamber. A simple frost heave testing method using a temperature-controllable cell has been proposed to overcome these difficulties, but it has not yet been established whether a temperature-controllable cell can adequately replace the ASTM International recommended apparatus. This paper reviews the applicability of the ASTM International testing method using the temperature-controllable cell. Freezing tests are compared using various soil mixtures with and without delivering blow to depress the freezing point (as recommended by ASTM International), and it is established that delivering blow does not affect heave rate, which is the key parameter in successful characterization of frost susceptibility. As the freezing temperature decreases, the duration of supercooling of pore water shortens or is eliminated; i.e., thermal shock with a sufficiently low freezing temperature can minimize or possibly eliminate supercooling.

**Keywords:** freezing temperature; frost heave; heave rate; standard testing method; supercooling

## 1. Introduction

When fine-grained soils are frozen, cryosuction (negative pore pressure) causes groundwater migration via freezing of in situ pore water and water entering from unfrozen soil or an external source and reaching the freezing front, forming an ice lens and causing frost heave (Konrad and Morgenstern 1980, 1981, Seto and Konrad 1994, Zheng *et al.* 2016, Jin *et al.* 2021c). Frost heave deforms soils and causes uneven uplift of the ground and geotechnical structures, and efforts to prevent damage rely on classifying the frost susceptibility of soils (Bilodeau *et al.* 2008, Sheng *et al.* 2013, Hendry *et al.* 2016). Advanced countries that consider frozen ground engineering, including the United Kingdom, Japan, and the United States, have developed their own laboratory testing apparatus to classify frost susceptibility (Jones 1980, JGS 2009, ASTM International 2013). Among them, the methodology of ASTM International (formerly the American Society for Testing and Materials) has the advantage of having been used to acquire much data internationally, making it a useful reference for evaluating the national standards for each country. However, ASTM International's methodology is expensive and complex,

requiring advanced expertise.

The Korea Institute of Civil Engineering and Building Technology (KICT) has recently developed simple frost heave testing apparatus that includes a temperature-controllable cell (Jin *et al.* 2019a, b). Jin *et al.* (2017, 2021a, b, 2022) used this simple apparatus to evaluate the reliability of the frost susceptibility classification criteria, investigate an engineering determination method of the segregation potential (SP), and assess the correlation between SP and hydraulic conductivity. Specifically, the SP, which is obtained from step-freezing frost heave tests of short duration (Konrad, 1988a) and is defined as the ratio of water intake rate ( $v(t)$ ) and overall temperature gradient in the frozen fringe ( $gradT$ ) suggested by Konrad and Morgenstern (1980, 1981, 1982), is widely accepted in engineering design and for frost heave predictions along with the ASTM International standard. The present work studied the feasibility of using the temperature-controllable cell to measure frost susceptibility following the methodology of ASTM International. It could be a monumental starting point for integrating the criteria of frost heave prediction and frost susceptibility classification derived from the two most widely used and accepted methods in frozen ground engineering using the temperature-controllable cell. This paper presents a slight modification of the testing procedure and its boundary conditions for using the temperature-controllable cell for assessment following the ASTM International methodology. In addition, the ASTM International frost heave testing method is carefully reviewed.

\*Corresponding author, Ph.D.

E-mail: tnt306@kict.re.kr

<sup>a</sup>Ph.D.

E-mail: hyunwoo.jin@kict.re.kr

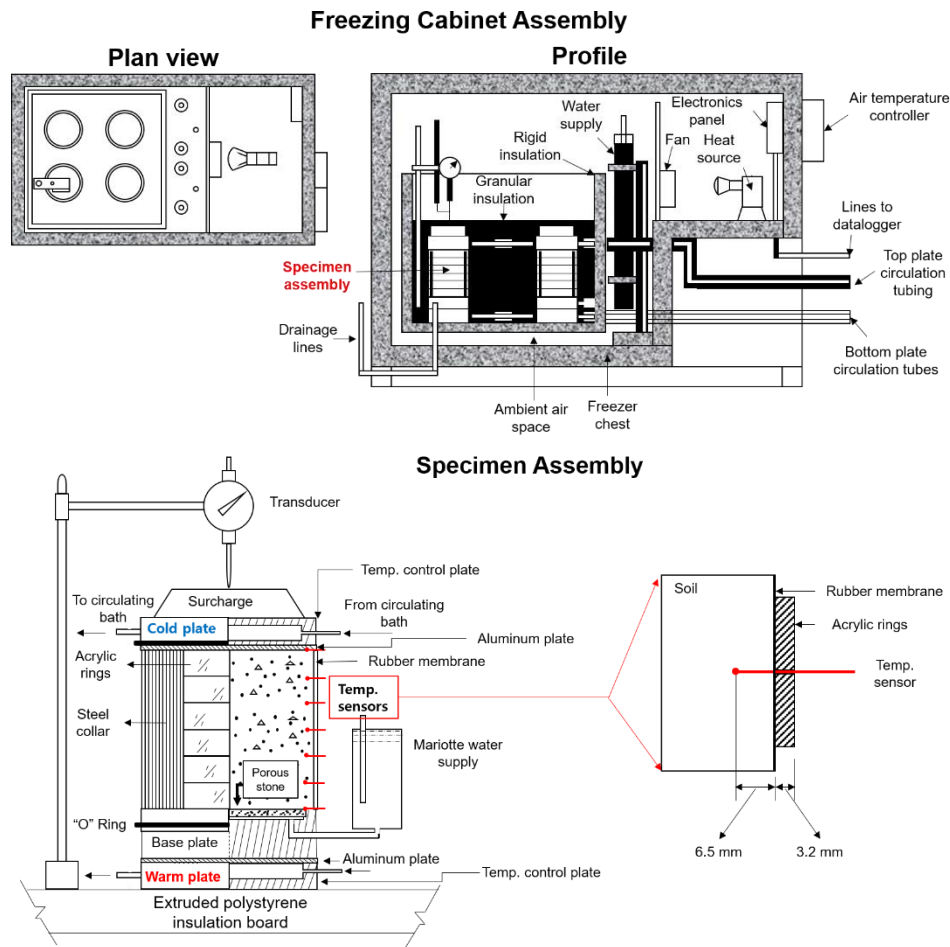


Fig. 1 ASTM International testing apparatus (ASTM International 2013)

## 2. Frost heave testing method

### 2.1 Compaction mold (ASTM International)

The method of ASTM International (Fig. 1) allows four soil specimens to be tested simultaneously by placing the specimen assemblies inside a freezing chamber with insulation between them. A chest freezer with 0.35 m<sup>3</sup> capacity is recommended to accommodate four test specimens, and the freezer should be able to maintain the ambient air around the specimen assemblies at  $2\pm 1.0^\circ\text{C}$ . Each specimen assembly (compaction mold) consists of a steel base plate, a hollow steel cylinder split longitudinally into three sections, two acrylic spacer disks, six acrylic rings, a steel collar, a rubber membrane, and four hose clamps. The six acrylic rings cover the soil specimen surrounded by the rubber membrane, and the steel collar restrains horizontal expansion. The temperature sensors must be small enough to permit their insertion into the soil specimen with minimal disturbance. Each specimen assembly is placed in the freezing chamber with top and bottom temperature control end plates, and a water supply during freezing is allowed through a drainage line connected to the bottom base plate (ASTM International, 2013).

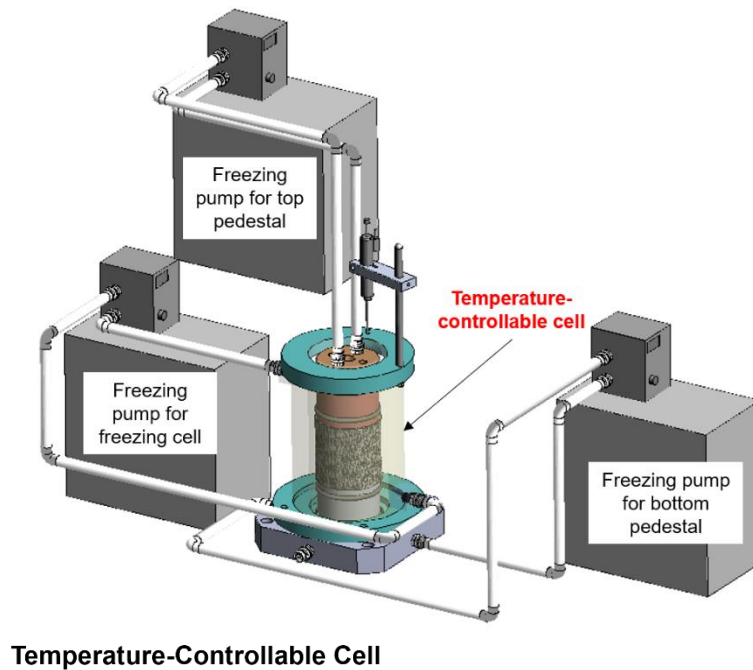
### 2.2 Temperature-controllable cell (KICT)

The frost heave testing apparatus developed by KICT consists of a temperature-controllable cell and three cooling pumps (Fig. 2). The cell is made of a transparent acrylic double tube (each 10 mm thick), and anti-freeze liquid is circulated between the tubes (15 mm gap) to control the temperature of the soil specimen's periphery. Controlling the peripheral temperature does not require an expensive freezing chamber, as it realizes one-dimensional freezing. Three cooling pumps are connected to independently control the temperature of the top, bottom, and periphery of the specimen. The specimen is located between the top and bottom pedestal with porous stones inside the cell. A temperature sensor module installed on the inner wall of the cell has 32 sensors at 5 mm intervals to measure temperatures across the soil specimen. Each temperature sensor has a measurement range of  $-40$  to  $+105^\circ\text{C}$  with  $\pm 0.5^\circ\text{C}$  accuracy (Jin *et al.* 2019a, 2021a, b, 2022).

### 2.3 Testing method modification

Table 1 compares the ASTM International and KICT frost heave testing methods. One-dimensional freezing is simulated in the ASTM International and KICT testing

### KICT Frost Heave Testing Apparatus



### Temperature-Controllable Cell

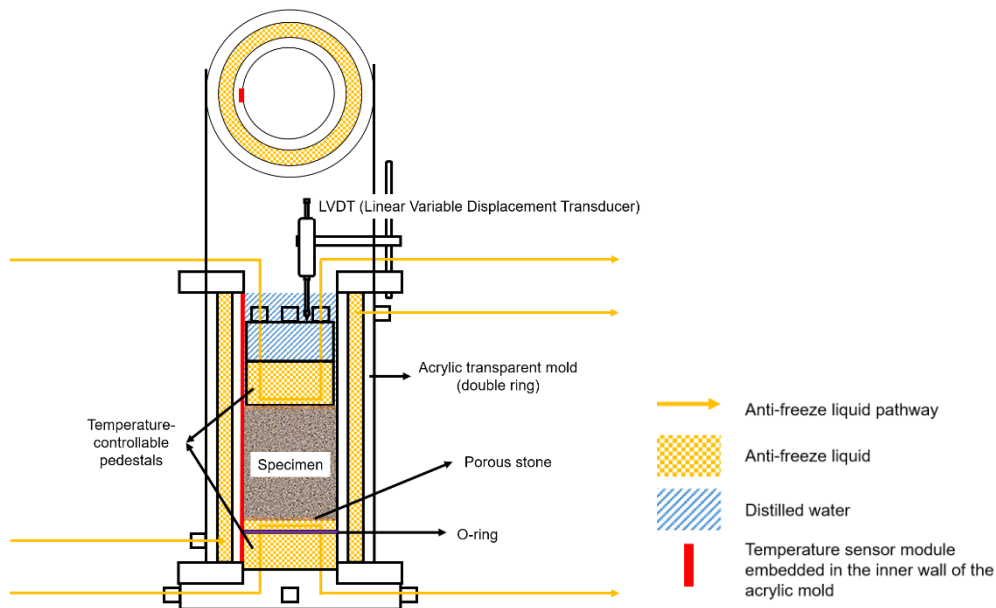


Fig. 2 KICT frost heave testing apparatus (Jin *et al.* 2019a, 2021a, b, 2022)

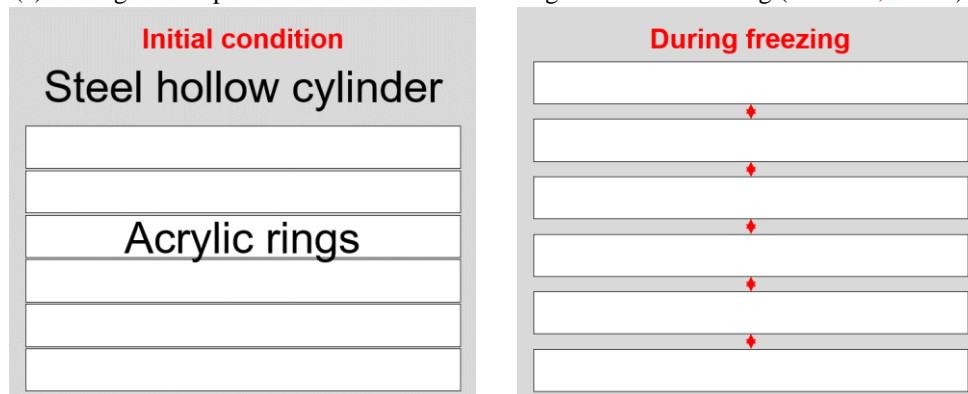
methods through peripheral insulation and peripheral temperature control, respectively. Both methods facilitate measurement of the frost heave amount (vertical displacement) on the top pedestal and the temperature profile across the soil specimen. Freezing is from the top downward for the ASTM International method, but from the bottom upward for the KICT method. When using a rigid wall mold made of such as acrylic, freezing from the top downward induces friction between the inner side wall of the mold and the frozen soil specimen, which lifts the mold upward. This side friction damages the connection between the mold and bottom pedestal (see Fig. 3(a)). To minimize its effect, the freezing direction is set from the bottom

upward (Konrad and Morgenstern 1982, Penner 1986, Konrad 1988a, b, 1989, 1994, Svec 1989). The ASTM International method encounters negligible side friction effects despite the soil specimens being frozen from the top downward, because the six acrylic rings can separate (see Fig. 3(b)).

Table 2 presents the boundary temperature conditions and tentative frost susceptibility classification criteria of the ASTM International method. ASTM International recommends that consistency of the results should be reviewed through two freeze–thaw cycles and that the heave rate obtained 8 h after freezing should be used for tentative frost susceptibility classification.

Table 1 Comparison of ASTM International and KICT testing methods

	ASTM International (ASTM International 2013)	KICT (Jin <i>et al.</i> 2019a, 2021a, b, 2022)
Freezing method	One-dimensional freezing	
Measurement	Vertical displacement, temperature	
Freezing direction	Top → bottom	Bottom → top
Water supply	Drainage line connected to external water supply reservoir	Soil specimen immersion
Specimen size	D = 146 mm, H = 150 mm	D = 100 mm, H = flexible
Temperature gradient for frost susceptibility classification	0.04 °C/mm	Flexible

(a) Damage to temperature-controllable cell during downward freezing (Jin *et al.*, 2019a)

(b) Splitting of the acrylic rings during frost heave

Fig. 3 Side friction between the mold and the frozen soil specimen

For freezing from the bottom upward, it is the unfrozen part that is pushed upward by the heaving soil. Therefore, as the height of the unfrozen part decreases, the side friction effect also decreases (Konrad, 1988a). In addition, one-dimensional heat flow can be easily simulated in laboratory specimens with small heights (i.e., <10 cm; Konrad 1994). For these reasons, this paper recommends using soil specimens with small heights. A soil specimen of ~50 mm high was frozen at around  $-1^{\circ}\text{C}$ , but a temperature gradient of  $\sim 0.04^{\circ}\text{C}/\text{mm}$  (similar to that of the ASTM International method) was applied as shown in Table 3. Using a similar temperature gradient causes similar formations of frozen fringe thickness and thus similar frost heave behavior as found in the previous studies (Fig. 4) (Jin *et al.* 2019c).

### 3. Frost heave tests

#### 3.1 Materials

Tested specimens were prepared from mixtures of sand (0.47 mm average particle size) and silt passed through a #200 sieve (0.075 mm). The particle size distribution curves of each component are shown in Fig. 5. Table 4 lists the properties of the sand and silt, including their classification as SP and ML, respectively, by the Unified Soil Classification System (USCS; ASTM International 2017a). Table 5 gives details of the five tested soil specimens (~100 mm diameter; ~50 mm height) made from the following mixtures of sand with 0%, 10%, 20%, 30%, and

Table 2 ASTM International frost heave testing conditions and frost susceptibility classification (ASTM International 2013)

Day	Elapsed time (h)	Top plate temperature (°C)	Bottom plate temperature (°C)	Comments
1	0	3	3	24 h conditioning
2	24	-3	3	First 8 h freezing
	32	-12	0	Freeze to bottom
3	48	12	3	First thaw
	64	3	3	
4	72	-3	3	Second 8 h freezing
	80	-12	0	Freeze to bottom
5	96	12	3	Second thaw
	112 to 120	3	3	

Tentative frost susceptibility criteria		
Frost susceptible classification	Symbol	8 h heave rate (mm/d)
Negligible	NFS	<1
Very low	VL	1 to 2
Low	L	2 to 4
Medium	M	4 to 8
High	H	8 to 16
Very high	VH	>16

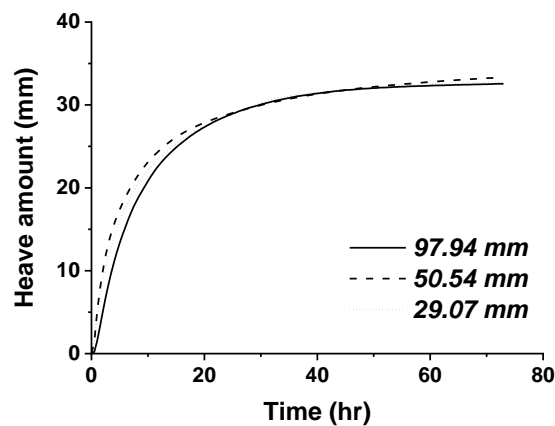
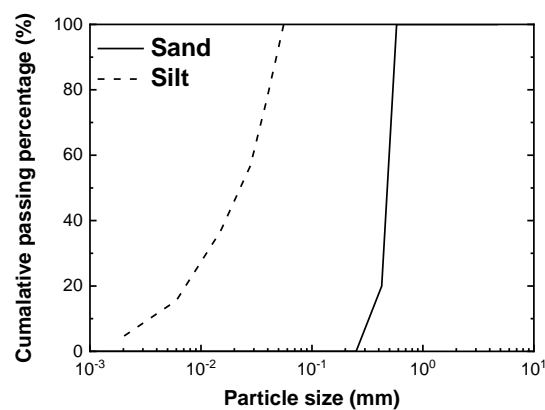
Fig. 4 Similar frost heave behavior using a similar temperature gradient with different sample height in previous study (Jin *et al.* 2019c)Fig. 5 Particle size distribution curves (Jin *et al.* 2020)

Table 3 Modified boundary temperature conditions using the temperature-controllable cell with soil specimens of ~50 mm height

Boundary temperature conditions				
Day	Elapsed time (h)	Top plate temperature (°C)	Bottom plate temperature (°C)	Comments
1	0	1	1	24 h conditioning
2	24	-1	1	First 8 h freezing
	32	-4	0	Freeze to bottom
3	48	4	1	First thaw
	64	1	1	
4	72	-1	1	Second 8 h freezing
	80	-4	0	Freeze to bottom
5	96	4	1	Second thaw
	112 to 120	1	1	

Table 4 Particle grading characteristics and soil classification (Jin *et al.* 2020)

Soil	*D <sub>10</sub>	*D <sub>30</sub>	*D <sub>60</sub>	Uniformity coefficient, $C_u$	Coefficient of curvature, $C_c$	Specific gravity, $G_s$	USCS
Joomunjin sand	0.36	0.44	0.51	1.42	1.05	2.65	SP
Crushed basalt	0.0076	0.03	0.1	13.16	1.18	2.94	ML

\*D<sub>n</sub>: The listed value is the diameter (mm) below which n% of particles are smaller

Table 5 Mixing ratios and initial conditions of soil mixtures

Specimen No.	Weight fraction (%)		Initial height (mm)	Dry density (g/cm <sup>3</sup> )
	Sand	Silt		
1	100	0	55	1.53
2	90	10	53	1.58
3	80	20	50	1.68
4	70	30	45	1.87
5	50	50	45	1.87

Table 6 Frost heave testing conditions

Blow delivery	Freezing condition	Initial condition		Temperature (°C)			Temperature gradient (°C/mm)
		Height (mm)	Dry unit weight ( $\gamma_d$ , g/cm <sup>3</sup> )	Initial	Freezing		
					Top	Bottom	
O	1 <sup>st</sup> freezing	50	1.68	1.04	0.91	-1.15	0.04
	2 <sup>nd</sup> freezing			1.04	0.88	-1.14	0.04
X	1 <sup>st</sup> freezing			1.05	0.88	-1.12	0.04
	2 <sup>nd</sup> freezing			1.04	0.87	-1.13	0.04

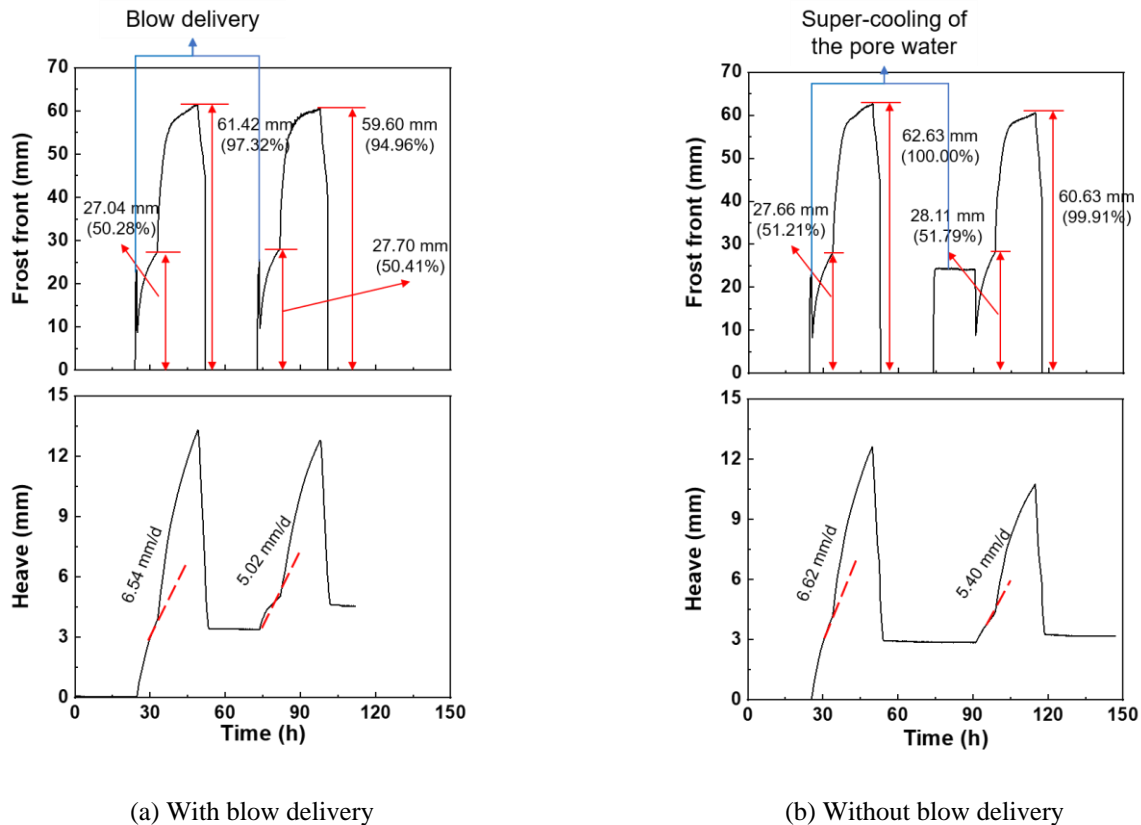
50% by weight of silt. The soil mixtures were reconstituted by air pluviation, dry tamping, and vibration. The initial height and dry density of the mixtures are also listed.

### 3.2 Testing conditions

Fully saturated soil specimens were prepared by injecting distilled water through the drainage line connected to the bottom pedestal and keeping distilled water above the specimen. This seepage boundary condition was adjusted to be hydrostatic and was maintained for 24 h. During freezing, the bottom drainage line was closed, and the

distilled water exceeding the specimen height was used for the water supply. In this way, freezing from the bottom upward provided a water reservoir at the top, precluding the need for an additional water supply system. However, it is not possible to measure the amount of water supplied and the rate, but this disadvantage can be overcome by using the measured frost heave data (Konrad 1987, Jin *et al.* 2021a). A negligible surcharge load of 1.62 kPa was applied, induced by the top pedestal, which was filled with anti-freeze liquid.

The testing conditions of specimen No. 3 (80% sand and 20% silt by weight) is described here as a representative



(a) With blow delivery (b) Without blow delivery  
 Fig. 6 Frost front ( $0^{\circ}\text{C}$ ) advancements and heave amounts with and without blow delivery

example. The Appendix gives all other testing conditions and results. Table 6 shows that the conditioning temperature was kept constant at  $\sim 1^{\circ}\text{C}$ , and the freezing temperature for classifying frost susceptibility was set to approximately  $-1^{\circ}\text{C}$  for the bottom and  $1^{\circ}\text{C}$  for the top. The applied temperature gradient of  $\sim 0.04^{\circ}\text{C}/\text{mm}$  was similar to that of the ASTM International method. That is, the specimen height and freezing temperature were different, but the frozen fringe thickness was set to be similar to that of ASTM International to realize similar frost heave behavior (Jin *et al.* 2019c). To analyze the freezing point depression that may occur in response to the relatively high freezing temperature ( $-1^{\circ}\text{C}$ ), the frost heave tests were conducted with and without delivering sharp blow for ice nucleation initiation (JGS 2009, ASTM International 2013), and comparative analysis was conducted.

#### 4. Test results

Frost heave test results for specimen No. 3 (80% sand and 20% silt by weight) following the temperature gradient condition suggested by ASTM International (Table 2) with and without delivering blow are analyzed. The results are different in each case.

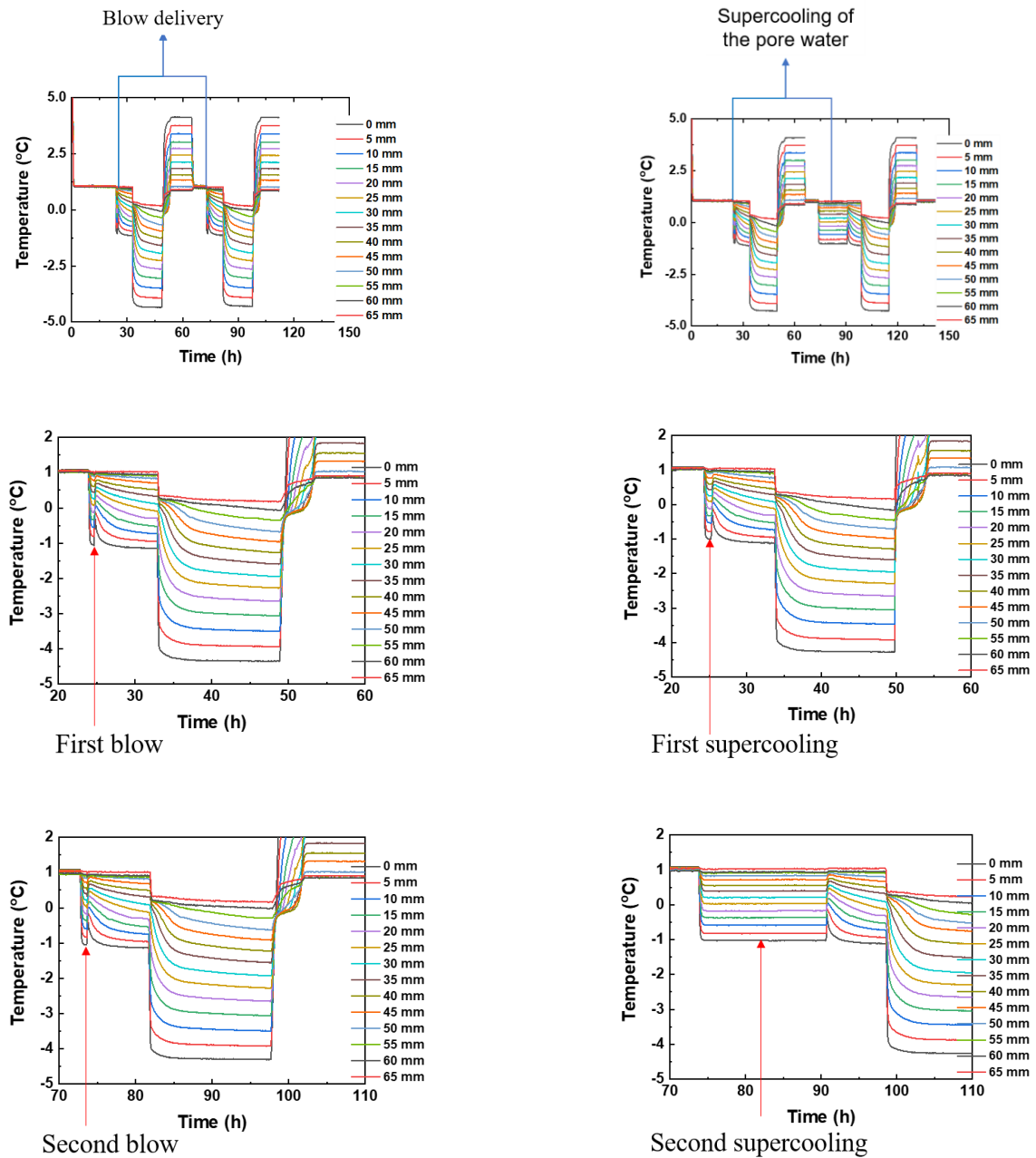
Delivering blow for  $\sim 1$  h after initiation of the first and second frost heave tests prevented a delay in freezing related to supercooling of the pore water and initiated ice nucleation. This is demonstrated by the advancement of the frost front ( $0^{\circ}\text{C}$ ). When the first and second frost heave tests

started, the frost front ( $0^{\circ}\text{C}$ ) advanced into the soil specimen from the bottom upward, reaching  $\sim 50\%$  of the soil specimen's height. When ice nucleation began, the frost front ( $0^{\circ}\text{C}$ ) withdrew from the bottom part of the specimen, and then advanced again when frost heave began. After the first 8 h of the frost heave test, the specimen was fully frozen ( $\sim 100\%$  of the soil specimen's height); it then thawed before the second frost heave test. At the end of first and second 8 h periods of freezing, the measured heave rates were  $\sim 6.54$  and  $5.02$  mm/d, respectively (Fig. 6(a)). In contrast, without delivering blow, supercooling of the pore water was observed as the frost front ( $0^{\circ}\text{C}$ ) stopped penetrating for  $\sim 1$  and  $\sim 17$  h after initiation of the first and second frost heave tests, respectively. When the ice nucleation began, the frost front ( $0^{\circ}\text{C}$ ) initially withdrew before advancing again. At the end of the first and second frost heave tests, the measured heave rates were  $\sim 6.62$  and  $5.40$  mm/d, respectively (Fig. 6(b)).

The heave rates measured in the first and second tests and used for frost susceptibility classification were similar to each other, both with and without delivering blow, even though the testing time was significantly affected by delivering blow because of the supercooling of pore water. The frost susceptibility of the soil specimen is classified as "medium" according to the tentative frost susceptibility criteria (ASTM International 2013) regardless of delivering blow. Table 7 lists the heave rate and frost susceptibility for the other soil specimens, which showed similar heave rates and were classified as having the same frost susceptibility regardless of delivering blow. As the silt content increased, the soils became increasingly frost susceptible.

Table 7 Heave rate and frost susceptibility measured following the ASTM International method

No.	With blow delivery				Without blow delivery			
	First		Second		First		Second	
	Heave rate (mm/d)	Frost susceptibility	Heave rate (mm/d)	Frost susceptibility	Heave rate (mm/d)	Frost susceptibility	Heave rate (mm/d)	Frost susceptibility
1	0.81	NFS	0.82	NFS	0.49	NFS	0.38	NFS
2	2.41	L	2.96	L	2.88	L	2.19	L
3	6.54	M	5.02	M	6.62	M	5.40	M
4	11.44	H	9.69	H	12.36	H	9.96	H
5	18.33	VH	17.18	VH	20.81	VH	16.73	VH



(a) With blow delivery

(b) Without blow delivery

Fig. 7 Temperature distribution curves with and without blow delivery

Table 8 Particle grading characteristics and soil classification

D <sub>10</sub>	D <sub>30</sub>	D <sub>60</sub>	Uniformity coefficient, C <sub>u</sub>	Coefficient of curvature, C <sub>c</sub>	Specific gravity, G <sub>s</sub>	USCS
0.06	0.11	0.44	7.33	0.46	2.56	SC

Table 9 Frost heave conditions for testing the effect of freezing temperature

No.	Initial condition		Temperature (°C)			Temperature gradient (°C/mm)	Blow delivery
	Height (mm)	Dry unit weight (V <sub>d</sub> , g/cm <sup>3</sup> )	Initial	Freezing			
				Top	Bottom		
1	51.2	1.41	0.98	0.92	-1.10	0.04	
2	52.2	1.38	2.04	1.75	-1.94	0.07	X
3	50.3	1.44	3.04	2.57	-3.05	0.11	

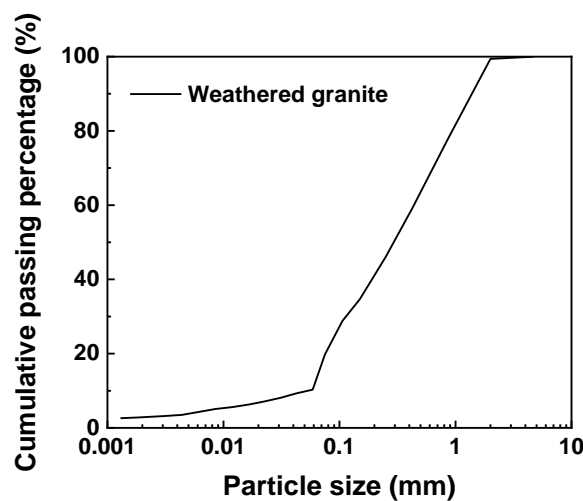


Fig. 8 Particle size distribution curve of weathered granite soil

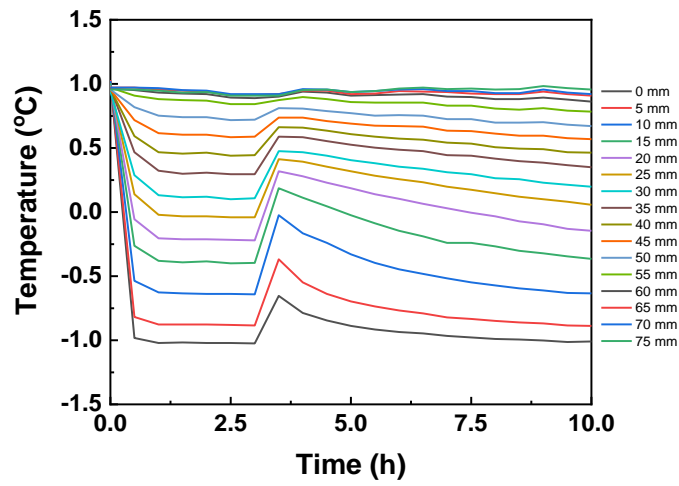
The initiation of ice nucleation can be better estimated using temperature distribution curves. In the case of delivering blow ~ 1 h after initiation of the frost heave tests, the temperature rose when ice nucleation began. Then, the temperature fell as the ice grew (Fig. 7(a)). Without delivering blow, a similar temperature fluctuation also occurred, but the duration of supercooling of the pore water was unpredictable (Fig. 7(b)). The first period of supercooling of the pore water lasted for only ~ 1 h, whereas the second was maintained for ~ 17 h. The Appendix presents the temperature distribution results with the heave rate included.

## 5. Freezing temperature effect

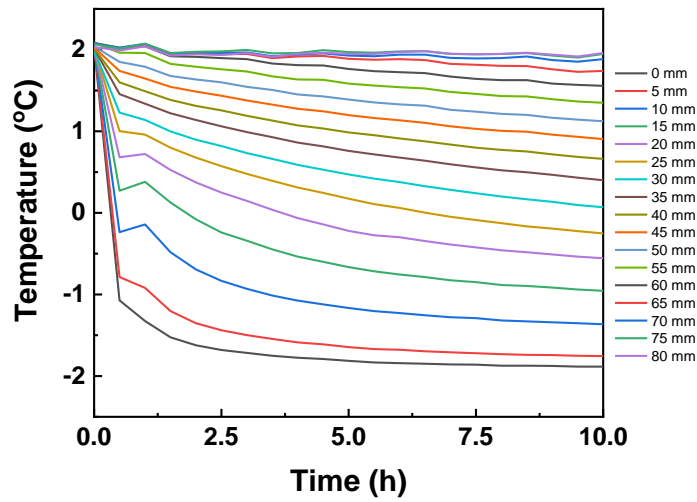
The test results confirmed that supercooling of the pore water occurred when the temperature gradient suggested by ASTM International was applied. Blow was delivered to eliminate the delay in freezing caused by supercooling of the pore water. However, it is uncertain whether supercooling can be avoided and the specimen may be disturbed during the process.

Additional frost heave tests were conducted to assess the effect of freezing temperature on ice nucleation. The particle size distribution curve is shown in Fig. 8; ~ 10.3% of the specimen could pass through a #200 sieve (0.075 mm). Table 8 lists weathered granite soil as SC by the USCS (ASTM International 2017a). Table 9 gives details of three tested soil specimens (~100 mm diameter) reconstituted by air pluviation, dry tamping, and vibration. To evaluate the effect of freezing temperature, freezing temperatures of approximately -1°C (temperature gradient ~ 0.04°C/mm), -2°C (temperature gradient ~ 0.07°C/mm), and -3°C (temperature gradient ~ 0.11°C/mm) were tested without delivering blow.

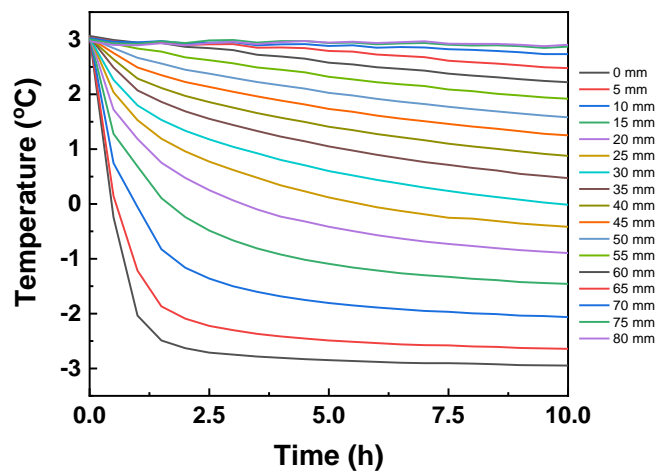
As a result, supercooling of the pore water was maintained for 2.5 and 1 h when freezing at approximately -1 and -2°C, respectively (Figs. 9(a) and 9(b)). However, no supercooling was observed for freezing at approximately -3°C (Fig. 9(c)). As the freezing temperature decreased, the duration of supercooling shortened. This result supports a previous finding that the probability of ice nucleation increases as the freezing temperature decreases (Gholaminejad and Hosseini 2013). The Japan Geotechnical Society's (JGS) standard method for laboratory testing



(a)  $-1^{\circ}\text{C}$



(b)  $-2^{\circ}\text{C}$



(c)  $-3^{\circ}\text{C}$

Fig. 9 Supercooling of pore water using different freezing temperatures

of the frost susceptibility of soils includes thermal shock to prevent supercooling of pore water. This method is commonly used to form ice nuclei by rapidly lowering the temperature. When ice formation begins, a slight increase in the specimen temperature and/or minor frost heave in the soil specimen are observed (JGS 0172 2009). To initiate ice nucleation by lowering the freezing temperature, the specimen height should increase to match the temperature gradient suggested by ASTM International.

## 6. Conclusions

This paper investigated the frost heave testing method of ASTM International using a temperature-controllable cell. Through this, the authors tried to find out whether the simple frost heave testing method using a temperature-controllable cell can adequately replace the expensive and laborious ASTM International standard testing method. Laboratory tests led to the following conclusions.

- The temperature-controllable cell can be used for frost heave tests following the method of ASTM International. Although the freezing direction and boundary temperature conditions need to be modified slightly, using the cell can make the procedure simpler and less costly.
- When the soil specimens were reconstituted, the first and second heave rates agreed well with each other. The frost heave testing results clearly show that the soil's frost susceptibility increased with increasing silt content.
- Regardless of whether delivering blow was applied to initiate ice nucleation, the experimental results for heave, heave rate, and temperature distribution obtained using the temperature-controllable cell were consistent. However, it is impossible to estimate the testing time without delivering blow, as the duration of supercooling is unpredictable. Supercooling can be minimized or possibly eliminated by delivering blow and by lowering the freezing temperature applied to maintain the temperature gradient.

## Acknowledgments

Research for this paper was carried out under the KICT Research Program (project no. 20220124, Development of Environmental Simulator and Advanced Construction Technologies over TRL6 in Extreme Conditions) funded by the Ministry of Science and ICT.

## References

ASTM International D2487 (2017a), Standard practice for classification of soils for engineering purposes (Unified Soil Classification System), ASTM International; West Conshohocken, PA, USA.

ASTM International D5918 (2013), Standard test methods for frost heave and thaw weakening susceptibility of soils, ASTM International; West Conshohocken, PA, USA.

ASTM International DD6913/D6913M (2017b), Standard test methods for particle-size distribution (gradation) of soils using sieve analysis, ASTM International; West Conshohocken, PA,

USA.

Bilodeau, J.P., Doré, G. and Pierre, P. (2008), "Gradation influence on frost susceptibility of base granular materials", *Int. J. Pavement Eng.*, **9**(6), 397-411. <https://doi.org/10.1080/10298430802279819>.

Gholaminejad, A. and Hosseini, R. (2013), "A study of water supercooling", *J. Elect. Cooling Therm. Contrl.*, **3**(1), 1-6. <https://doi.org/10.4236/jectc.2013.31001>.

Hendry, M.T., Onwude, L.U. and Sego, D.C. (2016), "A laboratory investigation of the frost heave susceptibility of fine-grained soil generated from the abrasion of a diorite aggregate", *Cold Reg. Sci. Technol.*, **123**, 91-98. <https://doi.org/10.1016/j.coldregions.2015.11.016>.

JGS 0172 (2009), Test method for frost susceptibility of soils, Japan Geotechnical Society; Tokyo, Japan.

Jin, H., Ryu, B.H. and Lee, J. (2022), "Assessment of the effect of fines content on frost susceptibility via simple frost heave testing and SP determination", *Geomech. Eng.*, **30**(4), 393-399. <https://doi.org/10.12989/gae.2022.30.4.393>.

Jin, H., Go, G.H., Ryu, B.H. and Lee, J. (2021c), "Experimental and numerical investigation of closure time during artificial ground freezing with vertical flow", *Geomech. Eng.*, **27**(5), 433-445. <https://doi.org/10.12989/gae.2021.27.5.433>.

Jin, H., Kim, I., Eun, J., Ryu, B.H. and Lee, J. (2021b), "Assessment of the correlation between segregation potential and hydraulic conductivity with fines fraction", *J. Korean Geotech. Soc.*, **37**(12), 47-56. <https://doi.org/10.7843/kgs.2021.37.12.47>.

Jin, H., Lee, J., Ryu, B.H. and Akagawa, S. (2019a), "Simple frost heave testing method using a temperature-controllable cell", *Cold Reg. Sci. Technol.*, **157**, 119-132. <https://doi.org/10.1016/j.coldregions.2018.09.011>.

Jin, H., Lee, J., Ryu, B.H., Shin, Y. and Jang, Y.E. (2019c), "Experimental assessment of the effect of frozen fringe thickness on frost heave", *Geomech. Eng.*, **19**(2), 193-199. <https://doi.org/10.12989/gae.2019.19.2.193>.

Jin, H., Lee, J., Zhuang, L. and Ryu, B.H. (2020), "Laboratory investigation of unconfined compression behavior of ice and frozen soil mixtures", *Geomech. Eng.*, **22**(3), 219-226. <https://doi.org/10.12989/gae.2020.22.3.219>.

Jin, H., Ryu, B.H. and Lee, J. (2017), "Evaluation on the reliability of frost susceptibility criteria", *J. Korean Geoenviron. Soc.*, **18**(12), 37-45. <https://doi.org/10.14481/jkges.2017.18.12.37>.

Jin, H., Ryu, B.H. and Lee, J. (2019b), "Experimental assessment and specimen height effect in frost heave testing apparatus", *J. Korean Geoenviron. Soc.*, **20**(1), 67-74. <https://doi.org/10.14481/jkges.2019.20.1.67>.

Jin, H., Ryu, B.H., Kang, J. and Lee, J. (2021a), "Engineering approach to determination of the segregation potential by the upward-step-freezing testing method", *Cold Reg. Sci. Technol.*, **191**, 103361-1-15. <https://doi.org/10.1016/j.coldregions.2021.103361>.

Jones, R.H. (1980), "Frost heave of roads", *Q. J. Eng. Geol.*, **13**(2), 77-86. <https://doi.org/10.1144/GSL.QJEG.1980.013.02.02>.

Konrad, J.M. (1987), "Procedure for determining the segregation potential of freezing soils", *Geotech. Geotech. Test. J.*, **10**(2), 51-58. <https://doi.org/10.1520/GTJ10933J>.

Konrad, J.M. (1988a), "Influence of freezing mode on frost heave characteristics", *Cold Reg. Sci. Technol.*, **15**, 161-175. [https://doi.org/10.1016/0165-232X\(88\)90062-6](https://doi.org/10.1016/0165-232X(88)90062-6).

Konrad, J.M. (1989), "Effect of freeze-thaw cycles on the freezing characteristics of a clayey silt at various overconsolidation ratios", *Can. Geotech. J.*, **26**, 217-226. <https://doi.org/10.1139/t89-031>.

Konrad, J.M. (1989b), "Influence of overconsolidation on the freezing characteristics of a clayey silt", *Can. Geotech. J.*, **26**, 9-21. <https://doi.org/10.1139/t89-002>.

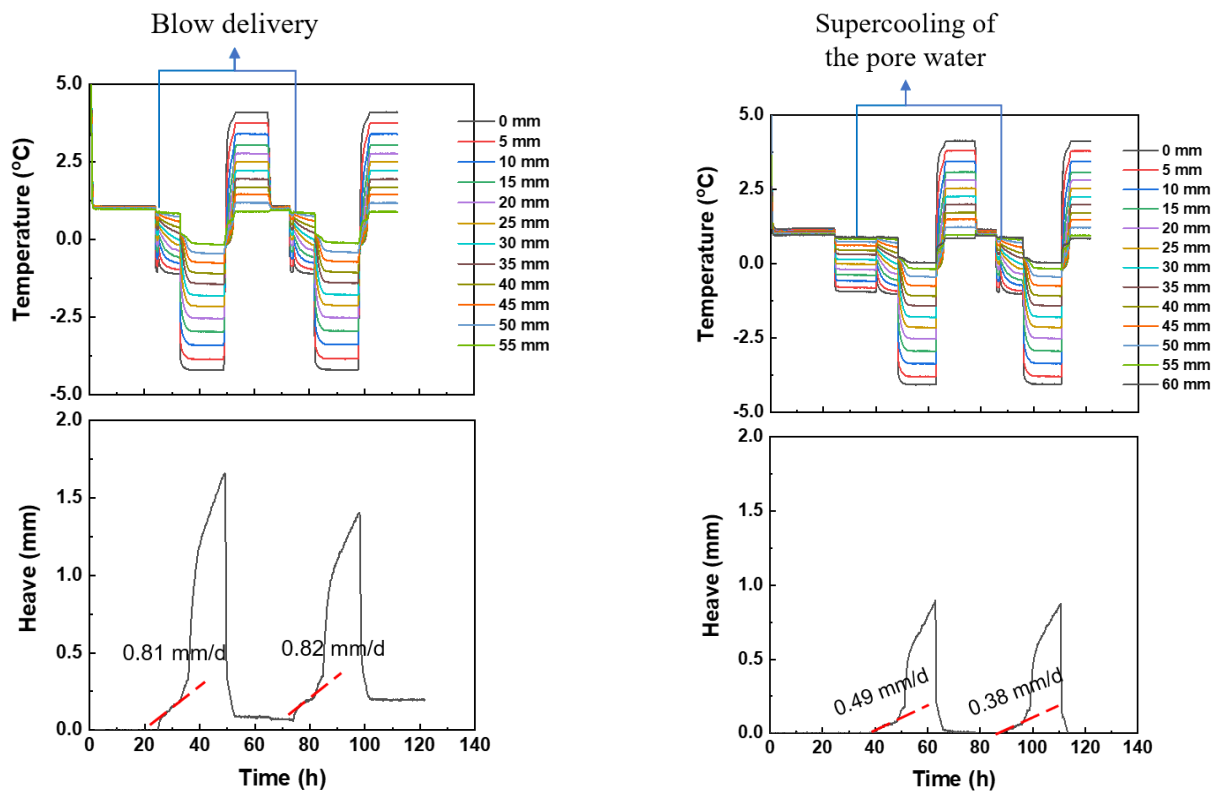
Konrad, J.M. (1994), "Sixteenth Canadian geotechnical

- colloquium: Frost heave in soils: Concepts and engineering”, *Can. Geotech. J.*, **31**, 223-245. <https://doi.org/10.1139/t94-028>.
- Konrad, J.M. and Morgenstern, N.R. (1980), “A mechanism theory of ice lens formation in fine-grained soils”, *Can. Geotech. J.*, **18**, 482-491. <https://doi.org/10.1139/t80-056>.
- Konrad, J.M. and Morgenstern, N.R. (1981), “The segregation potential of a freezing soil”, *Can. Geotech. J.*, **18**, 482-491. <https://doi.org/10.1139/t81-059>.
- Konrad, J.M. and Morgenstern, N.R. (1982), “Effects of applied pressure on freezing soils”, *Can. Geotech. J.*, **19**, 494-505. <https://doi.org/10.1139/t82-053>.
- Penner, E. (1986), “Aspects of ice lens growth in soils”, *Cold Reg. Sci. Technol.*, **13**, 91-100.
- Seto, J.T.C. and Konrad, J.M. (1994), “Pore pressure measurements during freezing of an overconsolidated clayey silt”, *Cold Reg. Sci. Technol.*, **22**, 319-338. [https://doi.org/10.1016/0165-232X\(94\)90018-3](https://doi.org/10.1016/0165-232X(94)90018-3).
- Sheng, D., Zhang, S., Yu, Z. and Zhang, J. (2013), “Assessing frost susceptibility of soils using PCHeave”, *Cold Reg. Sci. Technol.*, **95**, 27-38. <https://doi.org/10.1016/j.coldregions.2013.08.003>.
- Svec, O.J. (1989), “A new concept of frost-heave characteristics of soils”, *Cold Reg. Sci. Technol.*, **16**, 271-279. [https://doi.org/10.1016/0165-232X\(90\)90011-K](https://doi.org/10.1016/0165-232X(90)90011-K).
- Zheng, H. Kanie, S., Niu, F., Akagawa, S. and Li, A. (2016). “Application of practical one-dimensional frost heave estimation method in two-dimensional situation”, *Soils Found.*, **56**(5), 904-914. <https://doi.org/10.1016/j.sandf.2016.08.014>.

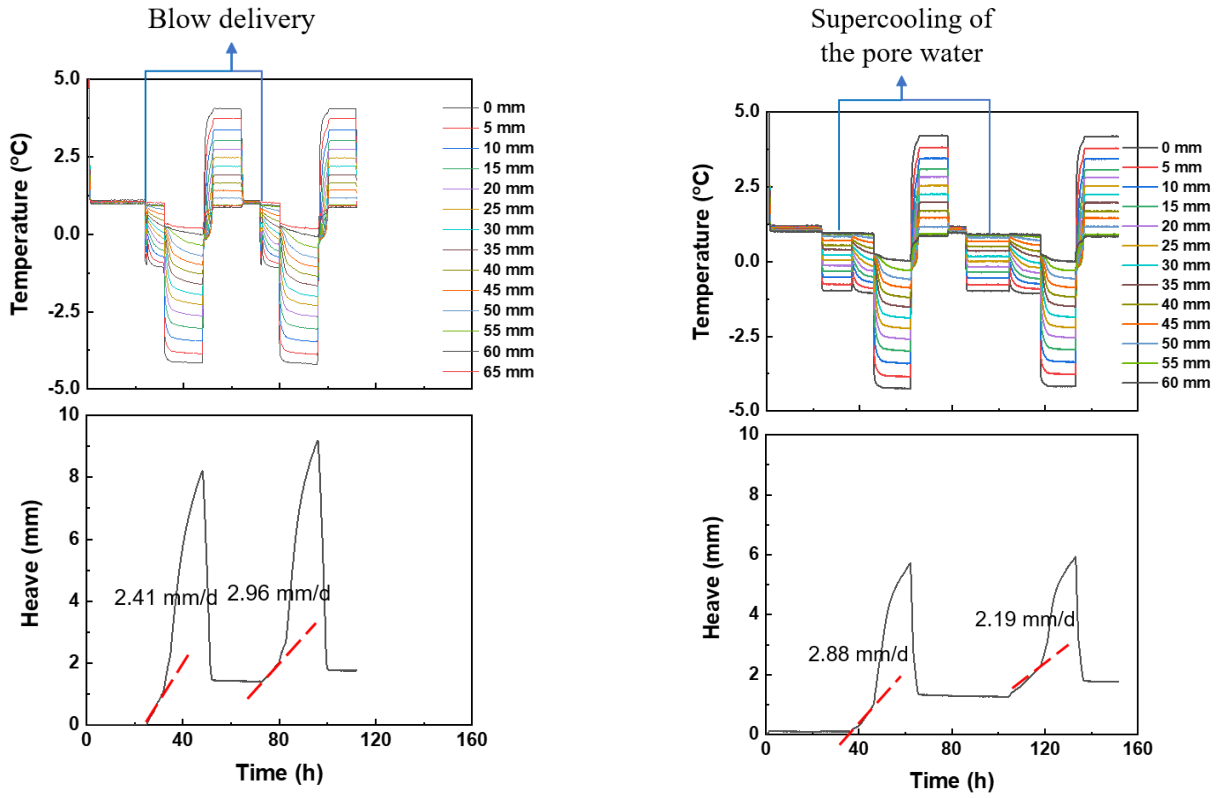
## Appendix I

## Frost heave testing conditions

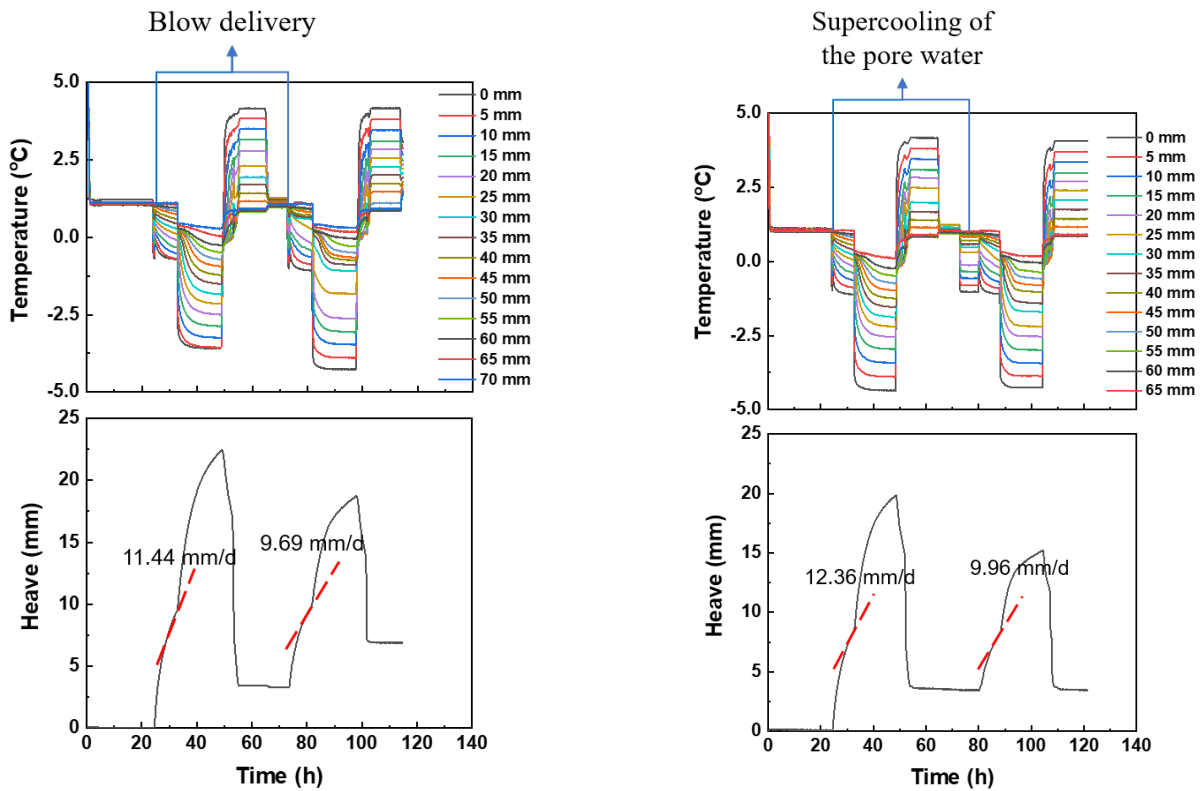
Specimen No.	Blow delivery	Freezing condition	Initial condition		Temperature (°C)			Temperature gradient (°C/mm)
			Height (mm)	Dry unit weight ( $\gamma_d$ , g/cm <sup>3</sup> )	Initial	Top	Bottom	
1	O	First freezing	55	1.53	1.04	0.84	-1.11	0.04
		Second freezing			1.04	0.84	-1.27	0.04
	X	First freezing			1.08	0.82	-1.01	0.03
		Second freezing			1.06	0.81	-1.01	0.03
2	O	First freezing	53	1.58	1.04	0.88	-1.01	0.04
		Second freezing			1.04	0.89	-1.08	0.04
	X	First freezing			1.09	0.88	-1.05	0.04
		Second freezing			1.07	0.85	-1.07	0.04
4	O	First freezing	45	1.87	1.10	0.93	-1.16	0.04
		Second freezing			0.93	0.91	-1.08	0.04
	X	First freezing			1.06	0.89	-1.12	0.04
		Second freezing			1.09	0.87	-1.10	0.04
5	O	First freezing	45	1.87	1.10	1.07	-1.01	0.03
		Second freezing			1.09	0.99	-1.07	0.04
	X	First freezing			1.10	0.87	-1.05	0.03
		Second freezing			1.08	0.87	-1.10	0.04



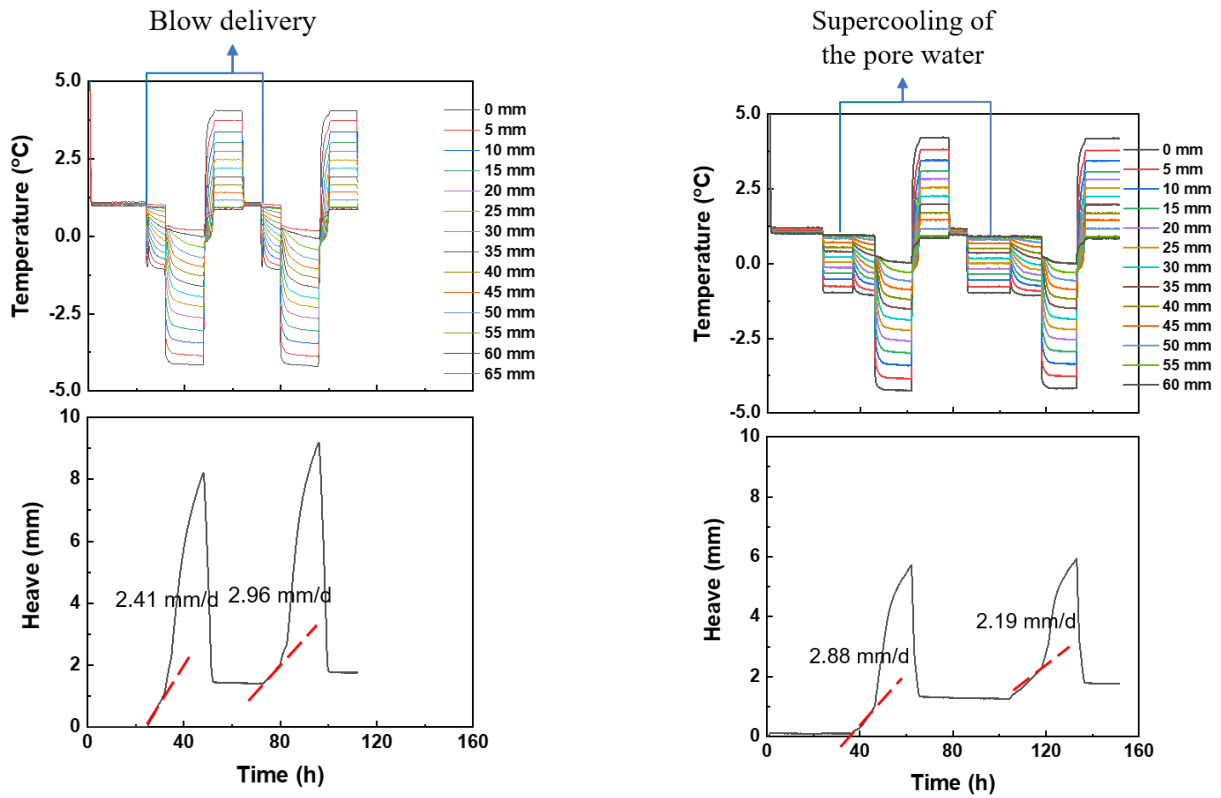
(a) Specimen No. 1 (100 wt.% sand)



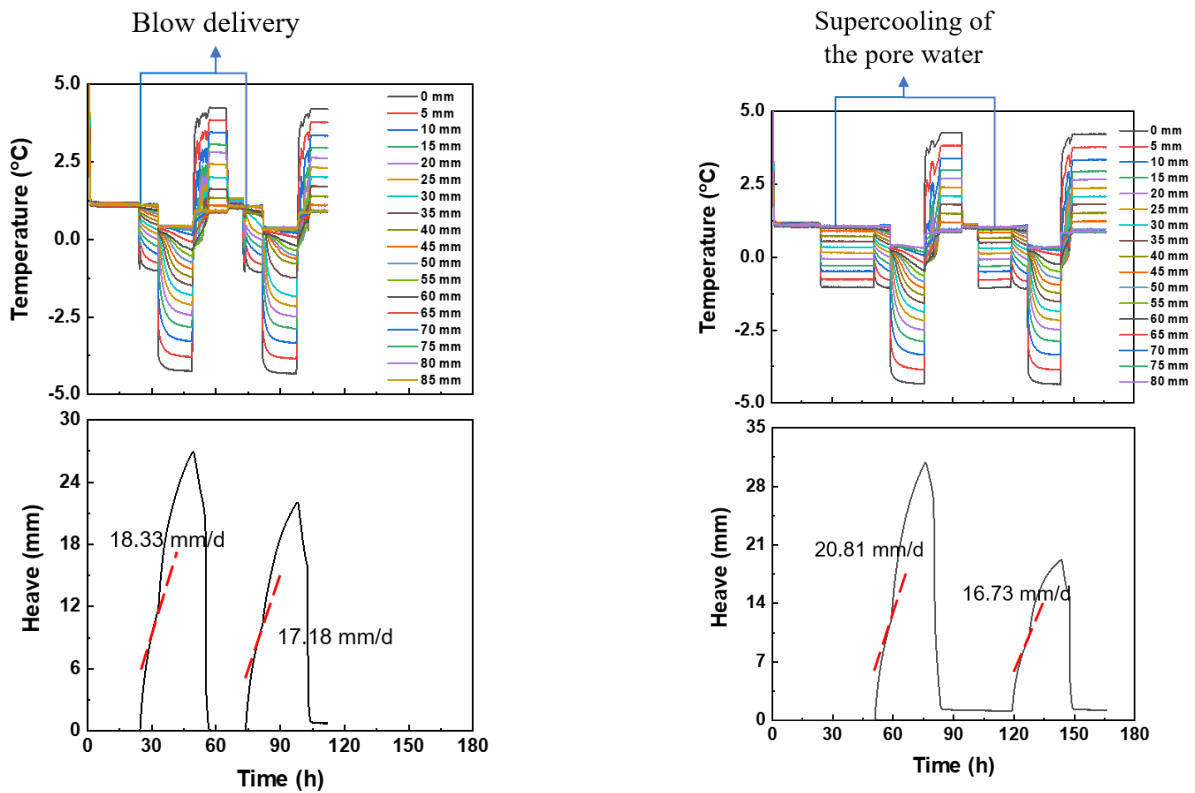
(b) Specimen No. 2 (90 wt.% sand + 10 wt.% silt)



(c) Specimen No. 4 (70 wt.% sand + 30 wt.% silt)



(b) Specimen No. 2 (90 wt.% sand + 10 wt.% silt)



(d) Specimen No. 5 (50 wt.% sand + 50 wt.% silt)

Temperature distribution and heave rate with and without blow delivery